Journal Pre-proof

TRPC3 Antagonizes Pruritus in A Mouse Contact Dermatitis Model

Katherine Beattie, Haowu Jiang, Mayank Gautam, Mary K. MacVittie, Barbara Miller, Minghong Ma, Qin Liu, Wenqin Luo

PII: S0022-202X(21)02222-3

DOI: https://doi.org/10.1016/j.jid.2021.08.433

Reference: JID 3126

To appear in: *The Journal of Investigative Dermatology*

Received Date: 24 May 2021

Revised Date: 27 July 2021

Accepted Date: 16 August 2021

Please cite this article as: Beattie K, Jiang H, Gautam M, MacVittie MK, Miller B, Ma M, Liu Q, Luo W, TRPC3 Antagonizes Pruritus in A Mouse Contact Dermatitis Model, *The Journal of Investigative Dermatology* (2021), doi: https://doi.org/10.1016/j.jid.2021.08.433.

This is a PDF file of an article that has undergone enhancements after acceptance, such as the addition of a cover page and metadata, and formatting for readability, but it is not yet the definitive version of record. This version will undergo additional copyediting, typesetting and review before it is published in its final form, but we are providing this version to give early visibility of the article. Please note that, during the production process, errors may be discovered which could affect the content, and all legal disclaimers that apply to the journal pertain.

© 2021 The Authors. Published by Elsevier, Inc. on behalf of the Society for Investigative Dermatology.

Journal Pre-proof

TRPC3 Antagonizes Pruritus in A Mouse Contact Dermatitis Model

Katherine Beattie[1], Haowu Jiang[2], Mayank Gautam[1], Mary K. MacVittie[1], Barbara Miller[3], Minghong Ma[1], Qin Liu[2], and Wenqin Luo[1*].

[1] *Department of Neuroscience, Perelman School of Medicine, University of Pennsylvania, Philadelphia, PA*

[2] *Center for the Study of Itch, Washington University at St. Louis School of Medicine, St. Louis, Missouri*

[3] *Department of Pediatrics, The Pennsylvania State University College of Medicine, Hershey, Pennsylvania*

**Correspondence: Wenqin Luo, wluo@pennmedicine.upenn.edu*

Twitter handle for Katherine Beattie: @*kbeattieneuro*

Short Title: Role of TRPC3 in Contact Dermatitis

Abbreviations: ACD, Allergic contact dermatitis; CD, contact dermatitis; CFA, Complete Freund's Adjuvant; CKO, conditional knock out; DRG, dorsal root ganglion; ICD, Irritant contact dermatitis; MRGPRs, Mas-related G-protein-coupled receptors; NP, non-peptidergic; SADBE, squaric acid dibutylester; SC, spinal cord; TRPC, transient receptor potential channel subfamily C.

Journal Pre-proof

Journal Pre-proof

Abstract

Contact dermatitis (CD), including allergic and irritant CD, are common dermatological diseases and characterized by an erythematous rash and severe itch. In this study, we investigated the function of TRPC3, a canonical TRP channel highly expressed in type 1 non-peptidergic (NP1) nociceptive primary afferents and other cell types, in a mouse CD model. Though *TrpC3* null mice had little deficits in acute somatosensation, they showed significantly increased scratching with CD. In addition, *TrpC3* null mice displayed no differences in mechanic and thermal hypersensitivity in an inflammatory pain model, suggesting that this channel preferentially functions to antagonize CD-induced itch. Using dorsal root ganglia (DRG) and pan-immune-specific *TrpC3* conditional KO (CKO) mice, we determined that *TrpC3* in DRG neurons, but not in immune cells, is required for this phenotype. Furthermore, the number of MRGPRD^{+} NP1 afferents in CD-affected DRGs is significantly reduced in *TrpC3* mutant mice. Taken together, our results suggest that *TrpC3* plays a critical role in NP1 afferents to cope with CD-induced excitotoxicity, and that degeneration of NP1 fibers may lead to an increased itch of CD. Our study identified a role of *TrpC3* and NP1 afferents in CD pathology.

Key words:

Contact dermatitis, DRG, MRGPRD, non-peptidergic nociceptors, pruritus, TRPC3

Journal Pre-proof

Introduction

Contact dermatitis (CD) is a common group of skin diseases, which include irritant contact dermatitis (ICD) and allergic contact dermatitis (ACD) (Nosbaum et al., 2009). ICD is the clinical manifestation of a local inflammatory reaction of the skin following exposure to a physical or chemical agent (Ale and Maibach, 2014). In ACD, activation of memory T cells, by re-exposure to allergens, causes an inflammatory cascade that results in skin injury and enhanced itch (Kostner et al., 2017). Itch sensation is a hallmark and main complaint of patients with CD, which can lead to a negative cycle of scratching, skin excoriations, and even worse itch sensation. These symptoms significantly affect patients' quality of life. At present, treatment of CD and CD-induced itch is limited due to our incomplete knowledge of the molecular mechanisms and difficulty in identifying the exact offending agent.

CD-induced itch sensation is generated by interactions of the primary sensory afferents, the immune system, and the integumentary system in the periphery. External and internal pruritogens are detected by free nerve terminals in the skin, whose cell bodies are in the dorsal root ganglion (DRG) and trigeminal ganglion. The signals are then relayed through the spinal cord to the brain to generate the perception of "itch". The immune system plays a critical role in triggering pathological pruritus by releasing inflammatory mediators that can directly activate pruitoceptors (Storan et al., 2015). Keratinocytes, the resident epithelial cells which comprise the epidermis, promote chronic itch through both direct (barrier disruption allowing pruritogen entry) and indirect mechanisms (cytokine release) (Schwendinger-Schreck et al., 2015).

Transient receptor potential (TRP) channels in mammals comprise a superfamily of over 30 membrane-bound proteins that form tetrameric non-selective cation channels and function in a variety of sensory pathways, including itch sensation (Julius, 2013, Montell, 2011, Sun and Dong, 2016). Canonical TRP family members (TRPC) can function downstream of a G-protein

Journal Pre-proof

coupled receptor (GPCR) or as receptors by themselves (Chen et al., 2020). TRPC channels can integrate several types of intracellular signals into changes in membrane potential and calcium entry (Chen et al., 2020). Indeed, deregulation of TRPC channels can disrupt calcium homeostasis and lead to cell damage and neuronal death (Chen et al., 2020, Jeon et al., 2021).

TRPC3 is a TRPC family member that is highly expressed in DRG neurons (Dong et al., 2017, Luo et al., 2009, Quick et al., 2012). In addition, it is also expressed in Purkinje cells, cholinergic neurons, thalamic glutamatergic neurons, and immune cells (Wenning et al., 2011, Zeisel et al., 2018). Within DRG, *TrpC3* is mainly expressed in non-peptidergic (NP) nociceptors: highest in the NP1 primary afferents, marked by a GPCR MRGPRD, and followed by NP2 and NP3 primary afferents, which are marked by MRGPRA3 and a neuropeptide natriuretic polypeptide B (NPPB), respectively (Usoskin et al., 2015, Zeisel et al., 2018). NP1 is a polymodal afferent for sensing mechanical force, chemicals, and temperature, whereas NP2 and NP3 afferents are itch selective (Cranfill and Luo, 2021). Despite the high expression of *TrpC3* in nonpeptidergic DRG neurons, *TrpC3* null mice exhibited few deficits in a variety of behavioral tests for acute pain and itch sensation, mechanosensation, and thermosensation (Dong et al., 2017, Quick et al., 2012).

Here we examined the role of *TrpC3* in a mouse CD model, which is induced by repeated application of squaric acid dibutylester (SADBE). Though this model was initially established as an ACD model (Qu et al., 2015), a later study using this model also found ICD features, including that itch could be induced in the absence of lymphocytes and that SADBE could directly activate primary sensory neurons (Feng et al., 2017). In contrast to the minor deficits in acute somatosensory assays (Dong et al., 2017, Quick et al., 2012), *TrpC3* null mice displayed a significant increase in spontaneous scratching of this SADBE-CD model, suggesting that TRPC3

functions to antagonize CD-induced itch. We generated DRG neuron and immune cell specific *TrpC3* CKO models and found that *TrpC3* in DRG is required for this phenotype. Moreover, we performed immunohistochemistry with the DRG, skin, and spinal cord of affected and unaffected regions of control and *TrpC3* null mice and revealed a significant reduction in the number of MRGPRD^{+} NP1 nociceptors innervating the affected region of mutant mice. Since TRPC3 is a known mediator of calcium homeostasis and plays a critical role in excitotoxicity (Alkhani et al., 2014, Jeon et al., 2021), we propose a model that *TrpC3* null MRGPRD^{+} NP1 nociceptors are susceptible to excitotoxicity induced by this CD model and that degeneration of NP1 neurons somehow disinhibits the itch pathway, resulting in an increased amount of scratching in *TrpC3* mutant mice.

Results

TrpC3 antagonizes scratching behavior in a mouse CD model

Given the high expression of *Trpc3* in DRG neurons, it was surprising that almost no behavioral deficits in acute sensation were identified in *TrpC3* null mice (Dong et al., 2017, Hirschler-Laszkiewicz et al., 2012). To further explore its function in somatosensation, we examined *TrpC3* null mice using a CD model (Qu et al., 2014). Briefly, adult male and female *TrpC3* null and wild type (WT) control mice were treated with SADBE on their abdomens and then re-challenged with SADBE at their necks after a week. Their spontaneous behavior was recorded and quantified on Day 16 (Figure 1a). As described before (Dong et al., 2017, Hirschler-Laszkiewicz et al., 2012), the *TrpC3* null allele was created by excision of exons 7 and 8 (Figure 1b), which encode the pore-defining region of the channel, resulting in a transcript with premature stop codon and non-functional TRPC3. SADBE treatment induced comparable ulcerative thickness and lymphocytic infiltration in WT and null mice (Figure 1d-f), suggesting

Journal Pre-proof

Journal Pre-proof

that the absence of TRPC3 did not impede the typical skin pathology associated with the CD model. Interestingly, knocking out *TrpC3* resulted in a marked increase in spontaneous scratching bouts, an itch-indicating behavior, in two independent cohorts from laboratories at Washington University (Cohort W) and the University of Pennsylvania (Cohort P) (Figures 1g-h). The average scratching bout numbers in the Cohort P were higher than that in Cohort W because this cohort excluded mice that were inactive for more than 50% of the 1-hour recording time (the same criterion was used for the following experiments). We further analyzed the scratching behavior by examining the average scratch duration per bout and the number of scratching bouts in 5-minute bins. No difference in bout duration was found between genotypes (Figure 1i), but a statistically significant increase in the high scratching bout numbers/bin was seen in *TrpC3* null mice (Figure 1j-k). *TrpC3* null mice also displayed a marked increase in wiping behavior in this CD model (Figure 1j). In short, our results suggest the absence of functional TRPC3 may lead to an enhanced pathological itch in the SADBE-CD model.

Loss of TRPC3 does not alter mechanical allodynia, thermal hyperalgesia, or gait.

To determine whether *TrpC3* is also required in chronic inflammatory pain sensation, Complete Freund's Adjuvant (CFA) was injected in the hindpaw to induce inflammatory pain. Dynamic and static mechanical allodynia, as well as thermal sensitivity, were tested before and after CFA treatment. No significant differences were found for any of these behavioral assays (Figure 2a-c), suggesting that *TrpC3* is dispensable for modulating pain sensation in this inflammatory pain model. Of note, a *TrpC3* gain-of-function point mutation mouse line, Moonwalker (*Mwk)* mice, caused Purkinje cell degeneration and cerebellar ataxia (Becker et al., 2009). To test whether *TrpC3* null mice had the same deficit, we performed a footprint assay, measured their gait width,

Journal Pre-proof

Journal Pre-proof

and calculated the alternative coefficient. We found no statistically significant differences in gait width and alternative coefficient (Figure 2d-f). These results are consistent with our previous finding that *TrpC3* null mice displayed normal motor coordination on the rotarod assay (Dong et al., 2017). Taken together, these findings highlight the preferential requirement of *TrpC3* in modulating CD-induced scratching behavior.

***TrpC3* in DRG neurons is required to antagonize CD-induced scratching**

Based on mouse skin single cell RNAseq data (Joost et al., 2020) and our own RT-PCR result, *TrpC3* is barely detected in the mouse skin. Thus, we focused on determining TRPC3 function in neuronal and immune cells in modulating CD-induced scratching. We generated *TrpC3* conditional knockout (CKO) mice by crossing a genetic allele, in which exons 7 and 8 were floxed by loxP sites (Hirschler-Laszkiewicz et al., 2012), with different Cre lines (Figure 3a). Given the high expression level of *TrpC3* in DRG neurons, we generated a CKO mouse line that specifically knocked out *TrpC3* expression in DRG nociceptors, including all NP afferents, using the $TrpV1^{Cre}$ mouse line (Figure 3b-c)(Cavanaugh et al., 2011). We then induced CD in control ($TrpC3^{f/f}$) and TrpV1-CKO ($TrpV1^{Cre};TrpC3^{f/f}$) mice. Interestingly, TrpV1-CKO mice showed a significant increase in scratching bouts when compared to control mice (Figure 3d). Similar to the null mice, the TrpV1-CKO mice scratched with a greater frequency than the control mice (Figure 3e-f) but displayed no difference in the average scratch bout duration (Figure 3g). The number of wiping bouts was not significantly changed in TrpV1-CKO mice (Figure 3h). These results indicate that *TrpC3* in DRG neurons is required for antagonizing CD-induced scratching.

***TrpC3* in immune cells is not required to modulate CD-induced scratching**

To determine TRPC3 function in the immune system, we knocked out *TrpC3* expression in pan-immune cells utilizing the *Vav1*^{iCre} line (Figure 4a) (Yang et al., 2008) and induced CD in control (*TrpC3*$^{f/f}$) and Vav1-CKO (*Vav1*^{iCre};*TrpC3*$^{f/f}$) mice. No differences in spontaneous scratching behavior (including bout number, duration per bout, and frequency) or wiping were found between the genotypes (Figure 4b-d). These findings are consistent with the histological result: similar amount of inflammatory cell infiltration in affected skin of *TrpC3* null and WT mice (Figure 1d-f). Together, our data suggest that *TrpC3* in the immune cells is not required to modulate scratching and/or skin inflammation in SADBE-induced CD (Figure 4b-f).

Degeneration of MRGPRD^{+} neurons in the CD-affected region of *TrpC3* null mice

To reveal potential mechanisms underlying the increased CD-induced itch sensation of *TrpC3* mutant mice, we performed immunohistochemistry with the DRG, skin, and spinal cord of the affected cervical region of control and *TrpC3* null mice. Since *TrpC3* shows a highly overlapped expression with *Mrgprd* (Dong et al., 2017), we utilized the *Mrgprd*$^{EGFP(+/-)}$ allele (Zylka et al., 2005) to visualize the NP1 afferents. We found a significant reduction in IB4^{+} (marker of NP1 neurons) and GFP^{+} DRG neurons and a reduction of GFP^{+} fibers innervating the lamina II of the spinal cord (Figure 5a-c). In contrast, the number and central terminals of peptidergic (CGRP^{+}) neurons, which normally had low expression level of *TrpC3*, did not differ between genotypes (Figure 5a-b). Though CGRP+ and GFP+ fibers normally innervate the epidermis layer of the skin (Zylka et al., 2005), both types of intraepidermal free nerve terminals were lost in the SADBE treated neck skin, and only few dermis innervating fibers remained. No significant difference was found in the number of these remaining dermis nerve fibers (Figure 5d).

Together, these results indicate that *TrpC3* null MRGPRD$^+$ NP1 neurons innervating the CD-affected skin region degenerate and die.

Since our previous data demonstrated a normal number of MRGPRD$^+$ DRG neurons and spinal cord and skin innervation in untreated juvenile *TrpC3* null mice (Dong et al., 2017), this result suggests either an age-dependent increase in cell death or an increased cell death caused by the SADBE-CD model. To differentiate the two possibilities, we conducted immunohistochemistry on lumbar DRGs that innervate the untreated mouse skin (Figure 6a). No differences in MRGPRD$^+$ neurons, nonpeptidergic (IB4), or peptidergic (CGRP) neurons were found (Figure 6b). This result suggests that the decrease in cervical MRGPRD$^+$ (NP1) neurons of *TrpC3* null mice is due to an increased cell death caused by the SADBE-CD model.

Discussion

In this study, we identified a function of TRPC3 in somatosensation: antagonizing pathological scratching of the SADBE-CD model, and determined that *TrpC3* in DRG neurons, but not in immune cells, is required for this function. Interestingly, in the affected region of *TrpC3* null mice, there is a marked reduction in the number of MRGPRD$^+$ DRG neurons, where *TrpC3* is normally expressed at the highest level. Based on these results, we propose a hypothetical model that *TrpC3* is highly expressed in NP1 neurons, which normally antagonize the skin inflammation (Zhang et al., 2021) and itch pathway mediated by NP2 and NP3 neurons (Figure 6c). Upon CD induction, NP1 neurons encounter excitotxity and degenerate in the absence of *TrpC3*, which leads to the disinhibition of the itch pathway and results in increased itch behaviors/sensation (Figure 6c).

Journal Pre-proof

TRPC3 is a non-selective cation channel which mediates calcium homeostasis and sensitization of primary nociceptors through its ability to engage in both receptor-operated calcium influx and in store-operated calcium entry (Alkhani et al., 2014). In addition, TRPC3 can be coupled to metabotropic glutamate receptors (Hartmann et al., 2008) and is required for IgG immune complex-induced excitation of DRG neurons (Qu et al., 2012). Disruptions in *TrpC3* expression or TRPC3 activity can lead to dysfunction of calcium homeostatis and cell death. A gain-of-function mutation of TRPC3 in *Mwk* mice led to increased intracellular Ca^{2+} concentration, which resulted in purkinje cell death and ataxia (Becker et al., 2009). An additional mouse model of spinocerebellar ataxia found that *TrpC3* was downregulated before the onset of neural degeneration (Lin et al., 2000). $MRGPRD^{+}$ (NP1) afferents innervating SADBE treated skin become hyperexcitable and display spontaneous firing (Qu et al., 2014). Since NP1 afferents have the highest level of *TrpC3* expression, 2-5 fold higher than its expression in NP2 and NP3 afferents (Zeisel et al., 2018), knocking out *TrpC3* should disrupt calcium homeostasis in NP1 afferents to the greatest extent. We speculate that a combination of increased calcium entry and a deficit of TRPC3 renders NP1 neurons susceptible to chronic excitotoxicity induced by SADBE-CD (and ultimately cell death) (Figure 6c).

MRGPRD is expressed in ~20% of mouse DRG neurons whose afferents form the densest innervation of the epidermis, specifically in the stratum granulosum (Zylka et al., 2005). $MRGPRD^{+}$ (NP1) neurons are polymodal and respond to noxious heat, mechanical pain, inflammatory pain, and pruitogens such as β-alanine (Abdus-Saboor et al., 2019, Cavanaugh et al., 2009, Liu et al., 2012, Shinohara et al., 2004). Unlike the NP1 subpopulation, NP2 (which express *Mrgpra3* and *Mrgprc11*) and NP3 (which express somatostatin, the interleukin-31 receptor A (*IL31r*), and *Nppb*) neurons predominantly mediate histaminergic and non-

histaminergic itch (Han et al., 2013, Liu et al., 2009, Mishra and Hoon, 2013). Some recent studies further highlighted the critical role of NP2^{+} and NP3^{+} afferents in mediating dermatitis-induced itch (Solinski et al., 2019, Wang et al., 2021, Zhu et al., 2017) . Though it is generally believed that the "pain" pathway antagonizes the "itch" pathway (Lagerström et al., 2010, Liu et al., 2010), whether the NP1 pathway could inhibit the NP2/NP3 itch pathway has not been directly tested and established. Our study revealed that *TrpC3* mutant mice had increased scratching but decreased number of NP1 neurons when challenged with the SADBE-CD model. A possible model to explain these data is that the NP1 pathway normally inhibits the NP2/NP3 itch pathway, so NP1 afferent degeneration leads to disinhibition of the itch pathway, resulting in an increased scratching phenotype. Future experiments will be needed to test and establish this model, including the direct manipulation of NP1 neuronal activities while stimulating NP2 and/or NP3 afferents. A recent study revealed NP1 fibers function in inhibiting mast cell activities and skin inflammation (Zhang et al., 2021), which is also consistent with our model. In addition to the degeneration of MRGPRD^{+} afferents, other cellular and molecular mechanisms could also contribute to this phenotype and warrant future investigation.

In summary, our study discovered a previously unreported function of TRPC3 in modulating itch sensation of a mouse CD model. The molecular and cellular mechanisms we identified here will help to understand the full pathology of CD and develop additional treatment strategies.

Materials and Methods

Mice

Three to four-month-old male and female mice were used for all behavioral and histology experiments. *TrpC3* null mice and floxed *TrpC3* mice were described as previously (Dong et al., 2017, Hirschler-Laszkiewicz et al., 2012). *Mrgd*^{EGFP} mice were obtained from Xinzhong Dong's

lab (Zylka et al., 2005). C57BL/6J (000664), *Trpv1^{Cre}* (017769), and *Vav1^{iCre}*(008610) mice were purchased from Jackson Laboratories (Cavanaugh et al., 2011, Yang et al., 2008). All experiments were conducted in accordance with the National Institute of Health guidelines and with approval from the Animal Care and Use Committee of University of Pennsylvania and Washington University School of Medicine. Mice were housed in a 12-hour light/dark cycle with food and water *ad libitum*.

Journal Pre-proof

Behavior

Contact dermatitis model

A murine model of contact dermatitis was produced with repeated topical application of 25 μl of squaric acid dibutyl ester (SADBE, 1% in acetone, Sigma, 339792) on shaved skin. The protocol timeline was adapted from previously described procedures as summarized in Figure 1 (Qu et al., 2014, Scott et al., 2002). On day 16, spontaneous behavior was recorded for 1 hour (23 hours after the treatment), and scored for scratching behavior, wiping behavior, and inactive periods by researchers blinded to mouse genotype. Scratching bouts were defined as an uninterrupted movement of the hindpaw directed at the treated site and ended when paws were placed on the floor, licked, or paused in the air for more than 1 second. A wipe was defined as a downward movement of the forepaw to the head/neck. Scratch frequency distribution graphs were made by dividing the 1-hour video into 5-minute bins, quantifying the number of bouts that occurred in each interval, and sorting the interval into bins based on bout number. Then the percentage of low (< 60 bouts/bin) and high (≥ 60 bouts/bin) scratch bins were calculated and compared. Experiments on two cohorts of mice were independently conducted at the Washington University of St. Louis (Cohort W) and the University of Pennsylvania (Cohort P).

Inflammatory pain behaviors

Either saline or 10 µl intraplantar injection of CFA (Sigma, St. Louis; 1:1 dilution with saline, final concentration 5µg/10 µl) was injected into the plantar skin of mice. Static and dynamic mechanical sensitivity using von Frey hair and paintbrush respectively, and radiant heat response latencies using Hargreaves apparatus prior to CFA injection and again on days 1, 7, 14, 21, and 28 post-CFA were measured (Cheng et al., 2017).

Gait

Footprint analysis of *TrpC3* null and WT naïve mice was performed with ink and analyzed for gait with and alternative coefficient as previously published (Becker et al., 2009). Gait width was measured as the average lateral distance between right and left step pairs. The alternative coefficient was calculated by determining the mean of the absolute value of 0.5 minus the ratio of right-left step distance to right-right step distance for every right-left step pair.

Hematoxylin and eosin staining, Imaging, and Quantification

On day 17, treated and untreated neck skin was collected and fixed overnight in 4% buffered paraformaldehyde at 4°C (Thermo Scientific, AAJ19943K2), serially dehydrated using ethanol and xylene. Tissue was paraffin embedded, sliced (5 µm), and collected on positively charged slides and dried overnight at room temperature. Slides were stained with Hematoxylin (Leica, 3801540) and Eosin (Leica, 3801600) using an automated stainer (Leica, Autostainer XL). Images were collected at 20X magnification utilizing brightfield microscopy. Cellular infiltration and ulcer thickness were analyzed in Fiji.

Journal Pre-proof

RT-PCR. ≥4-month-old mice were deeply anesthetized with CO_2 and DRGs, cerebellum, and spleen tissue were dissected under RNase free conditions. Tissue was mechanically homogenized, RNA was isolated using the RNeasy Micro Kit (Qiagen 74004), and cDNA was synthesized with oligo-dT primers using the SuperScript First-Strand Synthesis system (Invitrogen 18080051). RT-PCR was performed on cDNA with primers for *TrpC3* (forward primer CCTGGCTTTCATGATTGGCATGTTC for exon 6 and reverse primer CACTCACATCTCAGCACACTGGGG for exon 11).

Immunostaining

Mice were anesthetized with ketamine and xylazine and transcardially perfused with 4% PFA (in PBS) on day 16. Immunostaining was performed according to previously described protocol (Dong et al., 2017, Olson et al., 2017)). Cervical (C2-C5) and lumbar (L2-L5) DRG and spinal cord (SC) were dissected and post-fixed for 2-4 hours in 4% PFA at 4°C. Neck skin was dissected and post-fixed in 4% PFA O/N. All tissues were cryoprotected in 30% sucrose in PBS O/N at 4°C and embedded in OCT. DRG sections were sliced at 20μm, collected on Superfrost Plus slides, and dried O/N at room temperature. Neck skin and SC were sliced at 20 μm and 30 μm, respectively, and processed as floating sections. Primary antibodies used include chicken anti-GFP (1:2,000 (skin), 1:1,000 (SC, DRG); Aves, GFP-1020), rabbit anti-GFP (1:1,000, Invitrogen, A-11122), rabbit anti-CGRP (1:1,000; Immunostar, 24112), Guinea pig anti-VGLUT1 (1:1,000, Millipore, AB5905), and Alexa 594 conjugated IB4 (1:500; Life Sciences, I21413). Anti-GFP antibodies were used to label the expression of GFP in $Mrgprd^{EGFP}$ mice. Secondary antibodies (all 1:500) were Alexa 488 conjugated goat anti-chicken antibody (Invitrogen, A-11039), Alexa 594 conjugated goat anti-rabbit antibody (Invitrogen, A21207),

and Alexa 647 conjugated goat anti-guinea pig antibody (Jackson Immunoresearch, 106-605-003). Images were collected using a Leica SP5 confocal microscope.

Data Analysis

All data, except for frequency graphs and figure 2 graphs, are presented as mean ± standard error of mean (SEM) and analyzed with using two-tailed *t*-tests. Frequency graphs are presented as the mean percentage of low and high scratch bins and analyzed with Chi-squared tests. Figure 2 graphs were analyzed using two-way ANOVA. Statistical analysis was performed using GraphPad Prism. Differences were considered significant if $p < 0.05$.

Author ORCIDS

Katherine Beattie: 0000-0002-1055-4547

Haowu Jiang: 0000-0003-2477-5970

Mayank Gautam: 0000-0002-7257-5837

Mary K. MacVittie: 0000-0002-4794-643X

Barbara Miller: 0000-0002-9313-4686

Minghong H. Ma: 0000-0002-5027-9623

Qin Liu: 0000-0003-4333-4951

Wenqin Luo: 0000-0002-2486-807X

Conflict of Interest

The authors state no conflict of interest.

Journal Pre-proof

Journal Pre-proof

Acknowledgements

We thank members of Katherine's thesis committee for their advice, the Luo lab members for their help and support, and Dr. Phillip Scott and his lab members for immunology expertise. This work was supported by the National Institute of Health through grants from the NIAMS (F31 AR075436-01 to KB) and the NINDS (grant R01 NS083702 and R01NS094224 to WL). Histology research was supported by the Penn Skin Biology and Diseases Resource-based Center, funded by P30-AR069589.

Data Availability Statement

Datasets related to this article can be found at https://data.mendeley.com/datasets/hbrhfhfjj7/draft?a=c422df58-45aa-44a6-a1b7-ccccc6182b6a, hosted at Mendeley Data (Beattie, Katherine (2021), "TRPC3 Antagonizes Pruritus in A Mouse Contact Dermatitis Model", Mendeley Data, V1, doi: 10.17632/hbrhfhfjj7.1).

Author Contributions

Conceptualization: QL, WL, KB, HJ, MM; Data Curation: KB, HJ, MG, MKM; Data Analysis: KB, HJ, MG; Funding Acquisition: WL, KB; Investigation: KB, HJ, MG, MKM; Resources: WL, BM; Supervision: WL, QL; Validation: MKM, KB; Writing – Original Draft Preparation: KB, WL; Writing – Review and Editing: WL, KB, MM, BM, QL.

Journal Pre-proof

References

Abdus-Saboor I, Fried NT, Lay M, Burdge J, Swanson K, Fischer R, et al. Development of a Mouse Pain Scale Using Sub-second Behavioral Mapping and Statistical Modeling. Cell Rep 2019;28(6):1623-34.e4.

Ale IS, Maibach HI. Irritant contact dermatitis. Reviews on environmental health 2014;29(3):195-206.

Alkhani H, Ase AR, Grant R, O'Donnell D, Groschner K, Séguéla P. Contribution of TRPC3 to store-operated calcium entry and inflammatory transductions in primary nociceptors. Molecular Pain 2014;10:43-.

Becker EBE, Oliver PL, Glitsch MD, Banks GT, Achilli F, Hardy A, et al. A point mutation in TRPC3 causes abnormal Purkinje cell development and cerebellar ataxia in moonwalker mice. Proceedings of the National Academy of Sciences 2009;106(16):6706-11.

Cavanaugh DJ, Chesler AT, Jackson AC, Sigal YM, Yamanaka H, Grant R, et al. Trpv1 Reporter Mice Reveal Highly Restricted Brain Distribution and Functional Expression in Arteriolar Smooth Muscle Cells. The Journal of Neuroscience 2011;31(13):5067-77.

Cavanaugh DJ, Lee H, Lo L, Shields SD, Zylka MJ, Basbaum AI, et al. Distinct subsets of unmyelinated primary sensory fibers mediate behavioral responses to noxious thermal and mechanical stimuli. Proc Natl Acad Sci U S A 2009;106(22):9075-80.

Chen X, Sooch G, Demaree IS, White FA, Obukhov AG. Transient Receptor Potential Canonical (TRPC) Channels: Then and Now. Cells 2020;9(9).

Cheng L, Duan B, Huang T, Zhang Y, Chen Y, Britz O, et al. Identification of spinal circuits involved in touch-evoked dynamic mechanical pain. Nat Neurosci 2017;20(6):804-14.

Cranfill SL, Luo W. The development of somatosensory neurons: Insights into pain and itch. Current topics in developmental biology 2021;142:443-75.

Dong P, Guo C, Huang S, Ma M, Liu Q, Luo W. TRPC3 Is Dispensable for β-Alanine Triggered Acute Itch. Scientific Reports 2017;7(1):13869.

Feng J, Yang P, Mack MR, Dryn D, Luo J, Gong X, et al. Sensory TRP channels contribute differentially to skin inflammation and persistent itch. Nature Communications 2017;8(1):980.

Han L, Ma C, Liu Q, Weng H-J, Cui Y, Tang Z, et al. A subpopulation of nociceptors specifically linked to itch. Nature Neuroscience 2013;16(2):174-82.

Hartmann J, Dragicevic E, Adelsberger H, Henning HA, Sumser M, Abramowitz J, et al. TRPC3 Channels Are Required for Synaptic Transmission and Motor Coordination. Neuron 2008;59(3):392-8.

Hirschler-Laszkiewicz I, Zhang W, Keefer K, Conrad K, Tong Q, Chen S-j, et al. Trpc2 depletion protects red blood cells from oxidative stress-induced hemolysis. Experimental Hematology 2012;40(1):71-83.

Journal Pre-proof

Jeon J, Bu F, Sun G, Tian J-B, Ting S-M, Li J, et al. Contribution of TRPC Channels in Neuronal Excitotoxicity Associated With Neurodegenerative Disease and Ischemic Stroke. Frontiers in Cell and Developmental Biology 2021;8(1755).

Joost S, Annusver K, Jacob T, Sun X, Dalessandri T, Sivan U, et al. The Molecular Anatomy of Mouse Skin during Hair Growth and Rest. Cell stem cell 2020;26(3):441-57.e7.

Julius D. TRP channels and pain. Annual review of cell and developmental biology 2013;29:355-84.

Kostner L, Anzengruber F, Guillod C, Recher M, Schmid-Grendelmeier P, Navarini AA. Allergic Contact Dermatitis. Immunology and Allergy Clinics of North America 2017;37(1):141-52.

Lagerström MC, Rogoz K, Abrahamsen B, Persson E, Reinius B, Nordenankar K, et al. VGLUT2-dependent sensory neurons in the TRPV1 population regulate pain and itch. Neuron 2010;68(3):529-42.

Lin X, Antalffy B, Kang D, Orr HT, Zoghbi HY. Polyglutamine expansion down-regulates specific neuronal genes before pathologic changes in SCA1. Nature Neuroscience 2000;3(2):157-63.

Liu Q, Sikand P, Ma C, Tang Z, Han L, Li Z, et al. Mechanisms of itch evoked by β-alanine. The Journal of neuroscience : the official journal of the Society for Neuroscience 2012;32(42):14532-7.

Liu Q, Tang Z, Surdenikova L, Kim S, Patel KN, Kim A, et al. Sensory Neuron-Specific GPCR Mrgprs Are Itch Receptors Mediating Chloroquine-Induced Pruritus. Cell 2009;139(7):1353-65.

Liu Y, Abdel Samad O, Zhang L, Duan B, Tong Q, Lopes C, et al. VGLUT2-dependent glutamate release from nociceptors is required to sense pain and suppress itch. Neuron 2010;68(3):543-56.

Luo W, Enomoto H, Rice FL, Milbrandt J, Ginty DD. Molecular Identification of Rapidly Adapting Mechanoreceptors and Their Developmental Dependence on Ret Signaling. Neuron 2009;64(6):841-56.

Mishra SK, Hoon MA. The Cells and Circuitry for Itch Responses in Mice. Science 2013;340(6135):968-71.

Montell C. The history of TRP channels, a commentary and reflection. Pflügers Archiv - European Journal of Physiology 2011;461(5):499-506.

Nosbaum A, Vocanson M, Rozieres A, Hennino A, Nicolas JF. Allergic and irritant contact dermatitis. European journal of dermatology : EJD 2009;19(4):325-32.

Olson W, Abdus-Saboor I, Cui L, Burdge J, Raabe T, Ma M, et al. Sparse genetic tracing reveals regionally specific functional organization of mammalian nociceptors. Elife 2017;6.

Qu L, Fan N, Ma C, Wang T, Han L, Fu K, et al. Enhanced excitability of MRGPRA3- and MRGPRD-positive nociceptors in a model of inflammatory itch and pain. Brain 2014;137(4):1039-50.

Qu L, Fu K, Yang J, Shimada SG, LaMotte RH. CXCR3 chemokine receptor signaling mediates itch in experimental allergic contact dermatitis. PAIN 2015;156(9):1737-46.

Qu L, Li Y, Pan X, Zhang P, LaMotte RH, Ma C. Transient receptor potential canonical 3 (TRPC3) is required for IgG immune complex-induced excitation of the rat dorsal root ganglion neurons. J Neurosci 2012;32(28):9554-62.

Journal Pre-proof

Journal Pre-proof

Quick K, Zhao J, Eijkelkamp N, Linley JE, Rugiero F, Cox JJ, et al. TRPC3 and TRPC6 are essential for normal mechanotransduction in subsets of sensory neurons and cochlear hair cells. Open Biol 2012;2(5):120068-.

Schwendinger-Schreck J, Wilson SR, Bautista DM. Interactions Between Keratinocytes and Somatosensory Neurons in Itch. In: Cowan A, Yosipovitch G, editors. Pharmacology of Itch. Berlin, Heidelberg: Springer Berlin Heidelberg; 2015. p. 177-90.

Scott AE, Kashon ML, Yucesoy B, Luster MI, Tinkle SS. Insights into the Quantitative Relationship between Sensitization and Challenge for Allergic Contact Dermatitis Reactions. Toxicology and Applied Pharmacology 2002;183(1):66-70.

Shinohara T, Harada M, Ogi K, Maruyama M, Fujii R, Tanaka H, et al. Identification of a G Protein-coupled Receptor Specifically Responsive to β-Alanine. Journal of Biological Chemistry 2004;279(22):23559-64.

Solinski HJ, Kriegbaum MC, Tseng PY, Earnest TW, Gu X, Barik A, et al. Nppb Neurons Are Sensors of Mast Cell-Induced Itch. Cell Rep 2019;26(13):3561-73.e4.

Storan ER, O'Gorman SM, McDonald ID, Steinhoff M. Role of Cytokines and Chemokines in Itch. In: Cowan A, Yosipovitch G, editors. Pharmacology of Itch. Berlin, Heidelberg: Springer Berlin Heidelberg; 2015. p. 163-76.

Sun S, Dong X. Trp channels and itch. Seminars in immunopathology 2016;38(3):293-307.

Usoskin D, Furlan A, Islam S, Abdo H, Lönnerberg P, Lou D, et al. Unbiased classification of sensory neuron types by large-scale single-cell RNA sequencing. Nature Neuroscience 2015;18(1):145-53.

Wang F, Trier AM, Li F, Kim S, Chen Z, Chai JN, et al. A basophil-neuronal axis promotes itch. Cell 2021;184(2):422-40.e17.

Wenning AS, Neblung K, Strauß B, Wolfs M-J, Sappok A, Hoth M, et al. TRP expression pattern and the functional importance of TRPC3 in primary human T-cells. Biochimica et Biophysica Acta (BBA) - Molecular Cell Research 2011;1813(3):412-23.

Yang J, Hills D, Taylor E, Pfeffer K, Ure J, Medvinsky A. Transgenic tools for analysis of the haematopoietic system: Knock-in CD45 reporter and deletor mice. Journal of Immunological Methods 2008;337(2):81-7.

Zeisel A, Hochgerner H, Lönnerberg P, Johnsson A, Memic F, van der Zwan J, et al. Molecular Architecture of the Mouse Nervous System. Cell 2018;174(4):999-1014.e22.

Zhang S, Edwards TN, Chaudhri VK, Wu J, Cohen JA, Hirai T, et al. Nonpeptidergic neurons suppress mast cells via glutamate to maintain skin homeostasis. Cell 2021;184(8):2151-66.e16.

Zhu Y, Hanson CE, Liu Q, Han L. Mrgprs activation is required for chronic itch conditions in mice. Itch (Phila) 2017;2(3):e9.

Zylka MJ, Rice FL, Anderson DJ. Topographically Distinct Epidermal Nociceptive Circuits Revealed by Axonal Tracers Targeted to Mrgprd. Neuron 2005;45(1):17-25.

Journal Pre-proof

Journal Pre-proof

Figure Legends

Figure 1. *TrpC3* antagonizes scratching in the SADBE-CD model. **a.** Protocol and timeline of SADBE-induced CD model. **b.** Diagram of the *TrpC3* gene, depicting excision of exons 7–8 in null mice. **c.** Schematic representation of relative expression levels of *TrpC3* (based on mouse single neuron RNAseq data) in systems relevant to CD induced itch sensation. **d.** H & E staining of skin from SADBE-treated mice with dermal layers labeled: epidermis (E), dermis (D), ulcer (U). **e-f.** Quantification of ulcer thickness and cellular infiltration of treated neck skin ($\geq$10 measurements/mouse, *n*=3). **g-h.** Quantification of spontaneous scratch behavior of *TrpC3* null and WT mice on day 16 of the SADBE model (Cohort W, *n*=8 (males); Cohort P, WT *n*=10 (5 males, 5 females), *TrpC3* null *n*=8 (3 males, 5 females). **i.** Quantification of scratch duration per bout (s). **j.** Frequency distribution of scratch bout numbers in 5-minute bins. **k.** Bar graph comparing the percentage of low (<60 bouts) and high ($\geq$60 bouts) scratching bout bins. **l.** Quantification of wiping bouts**.** Scale bars = 50 µm. Student's two-tailed *t* test (e-i, l). Chi-squared test (k). ns, not significant. *Asterisks* indicate statistical significance. *p<0.05, **p<0.01; error bar, SEM.

Figure 2. Loss of TRPC3 does not alter mechanical allodynia, thermal hyperalgesia, or gait. Behavioral assays with WT and *TrpC3* null mice after CFA (*n*=7/genotype; 2 males, 5 females)

or saline (*n*=6/genotype; 1 male, 5 females) injection. **a.** 50% Paw withdrawal threshold (PWT) in response to von Frey filaments. **b.** Paw withdrawal score (PWS) in response to dynamic brush stimulation. **c.** Paw withdrawal latency (PWL) in Hargreaves test. **d.** Representative footprints of *TrpC*3 null and WT mice in gait assay. **e-f.** Quantification of gait width and the alternative coefficient (indicating step alternation uniformity) (*n*=5/genotype, females). Scale bar = 100 μm. Two-way ANOVA (a-c); Student's one-tail *t* test (e-f); error bar, SEM.

Journal Pre-proof

Figure 3. *TrpC3* is required in DRG neurons to antagonize CD-induced scratching.

a. Diagram of floxed *TrpC3* gene illustrating the loxP sites surrounding exons 7 and 8 of *TrpC3* gene and the location of the forward (FP) and reverse RT-PCR primers (RP). **b.** Schematic representation of knocking out *TrpC3* expression in DRG neurons**. c.** RT-PCR performed on RNA isolated from floxed control and TrpV1 CKO DRG, cerebellum, and spleen tissue. **d.** Quantification of scratch behavior of *TrpV1* CKO (*n* =9; 4 males, 5 females) and control mice on Day 16 (*n* =9; 5 males, 4 females). **e.** Frequency distribution of bout numbers in 5-minute bins. **f.** Bar graph comparing the total percentage of low (<60 bouts) and high (≥60 bouts) scratching bout bins. **g.** Quantification of scratch duration per bout (s). **h**. Quantification of wiping bouts. Student's two-tailed *t* test (b, e, f); Chi-squared test (d). *Asterisks* indicate statistical significance. **p<0.01; error bar, SEM.

Figure 4. *TrpC3* in immune cells is not required to modulate CD-induced scratching. a. Schematic illustration showing CKO of *TrpC3* from immune cells**. b.** Quantification of scratch bouts of *Vav1*-CKO and control mice on Day 16 (*n* =9; 4 males, 5 females/genotype). **c.** Quantification of scratch duration per bout (s). **d.** Frequency distribution of bout numbers in a 5-

minute bins. **e**. Bar graph comparing the percentage of low (<60 bouts) and high ($\geq$60 bouts) scratching bout bins. **f**. Quantification of wiping bouts**.** Student's two-tailed *t* test (c, d, g); Chi-squared test (f); error bar, SEM.

Figure 5. Degeneration of MRGPRD$^+$ neurons in the CD affected region of *TrpC3* null mice.

a. Immunostaining of adult *Mrgprd*$^{EGFP(+/-)}$ and *TrpC3* null; *Mrgprd*$^{EGFP(+/-)}$ mouse cervical DRG, spinal cord, and treated neck skin sections using IB4 and antibodies against CGRP and GFP. Skin layers: ulcer (U); dermis (D); subcutaneous layer (S). **b.** Quantification of marker positive DRG neuron numbers per section**. c.** Quantification of the innervation thickness of MRGPRD$^+$ central terminals. **d.** Quantification of dermal innervation of MRGPRD$^+$ fibers in 1000µm^2 area ($\geq$4 sections/mouse; *n*=3). Scale bars = 50 µm. Student's two-tailed *t* test. *Asterisks* indicate statistical significance. *p<0.05, ***p<0.001, ****p<0.0001; error bar, SEM.

Journal Pre-proof

Figure 6. MRGPRD$^+$ neurons are not affected in the control region of *TrpC3* null mice.

a. Immunostaining of adult *Mrgprd*$^{EGFP(+/-)}$ and *TrpC3* null; *Mrgprd*$^{EGFP(+/-)}$ mouse lumbar DRG, sections using IB4 and antibodies against CGRP and GFP. **b.** Quantification of marker positive DRG neuron numbers per section ($\geq$4 sections/mouse*, n*=3). **c.** Schematic of the hypothetical model of how TRPC3 functions in MRGPRD$^+$ neurons to antagonize CD-induced itch. Scale bars = 50 µm. Student's two-tailed *t* test.; error bar, SEM.

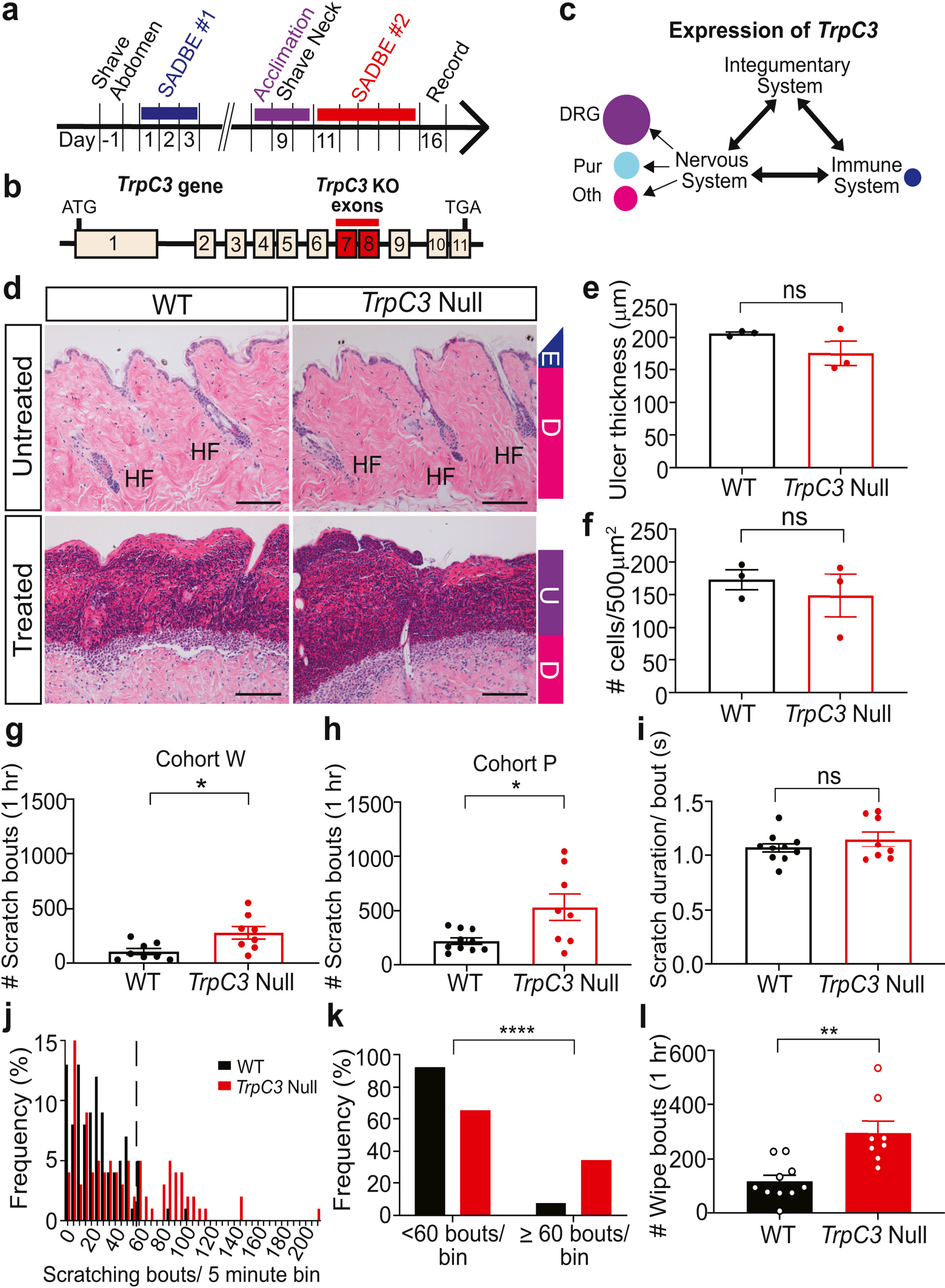
a
Day -1 1 2 3 9 11 16
Shave Abdomen
SADBE #1
Acclimation
Shave Neck
SADBE #2
Record
b
TrpC3 gene
TrpC3 KO exons
ATG
TGA
1 2 3 4 5 6 7 8 9 10 11
c
Expression of TrpC3
Integumentary System
Nervous System
Immune System
DRG
Pur
Oth
d
WT
TrpC3 Null
Untreated
Treated
HF
E
D
U
e
Ulcer thickness (µm)
ns
f
cells/500µm²
ns
g
Cohort W
Scratch bouts (1 hr)
*
h
Cohort P
*
i
Scratch duration/ bout (s)
ns
j
Frequency (%)
Scratching bouts/ 5 minute bin
k
Frequency (%)
****
<60 bouts/ bin
≥ 60 bouts/ bin
l
Wipe bouts (1 hr)
**
WT
TrpC3 Null

a Von Frey

ns

50% PWT (g)

1.5 1.0 0.5 0.0

BL CFA D1 D7 D14 D21 D28

b Dynamic Brush

ns

Mean PWS

4 3 2 1 0

BL CFA D1 D7 D14 D21 D28

c Hargreaves

ns

PWL (s)

10 8 6 4 2 0

BL CFA D1 D7 D14 D21 D28

WT CFA *TrpC3* Null CFA WT Saline *TrpC3* Null Saline

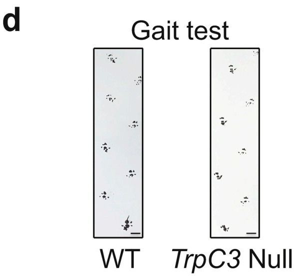

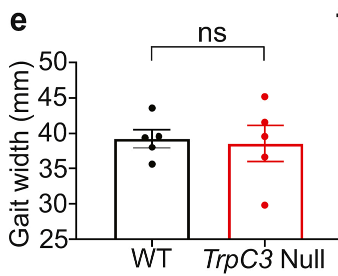

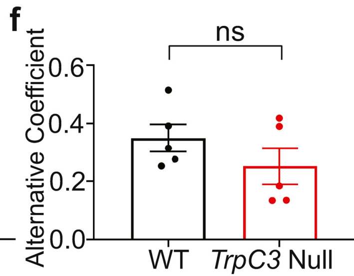

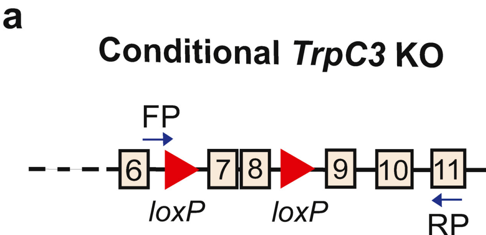
a
Conditional TrpC3 KO
FP
6
7
8
9
10
11
loxP
loxP
RP

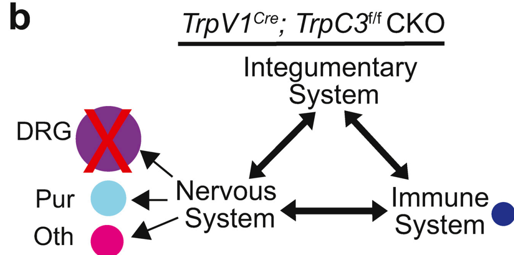
b
TrpV1Cre; TrpC3f/f CKO
Integumentary System
DRG
Pur
Oth
Nervous System
Immune System

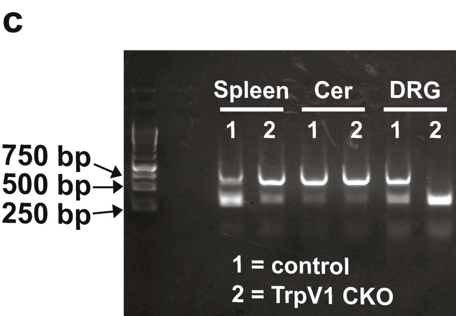
c
Spleen
Cer
DRG
1 2 1 2 1 2
750 bp
500 bp
250 bp
WT
KO
1 = control
2 = TrpV1 CKO

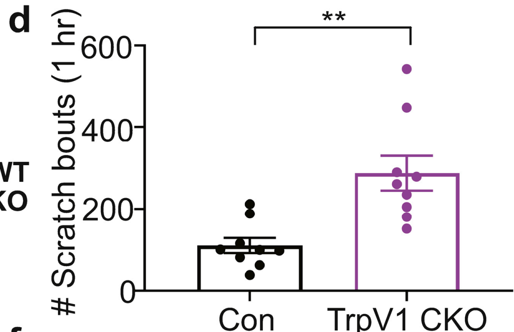
d
**
Scratch bouts (1 hr)
600
400
200
0
Con
TrpV1 CKO

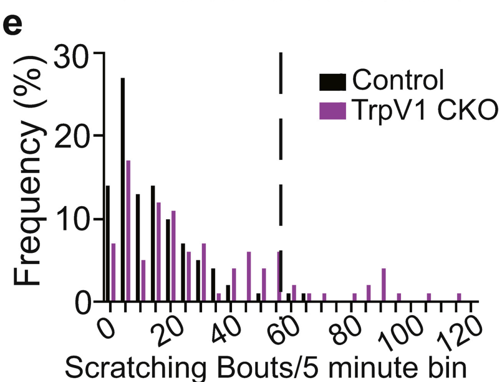
e
Frequency (%)
30
20
10
0
Control
TrpV1 CKO
0 20 40 60 80 100 120
Scratching Bouts/5 minute bin

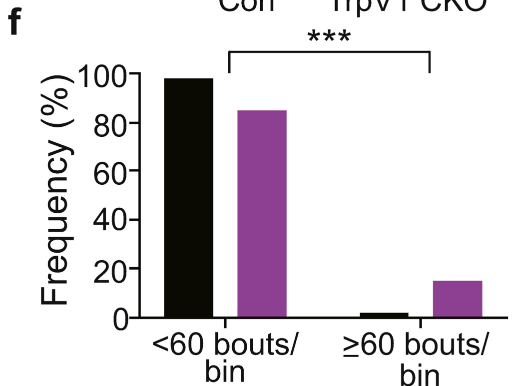
f
***
Frequency (%)
100
80
60
40
20
0
<60 bouts/ bin
≥60 bouts/ bin

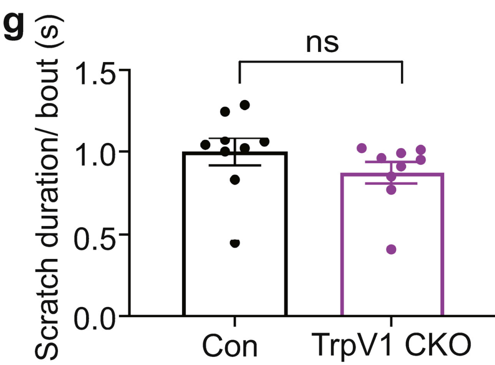
g
ns
Scratch duration/ bout (s)
1.5
1.0
0.5
0.0
Con
TrpV1 CKO

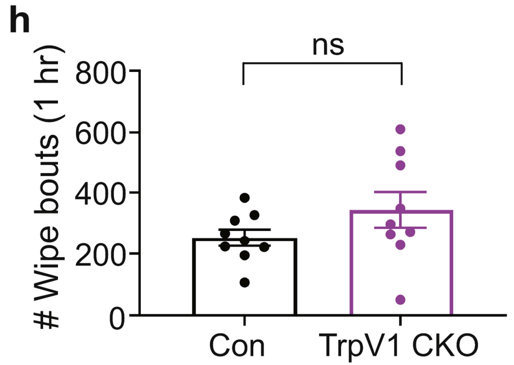
h
ns
Wipe bouts (1 hr)
800
600
400
200
0
Con
TrpV1 CKO

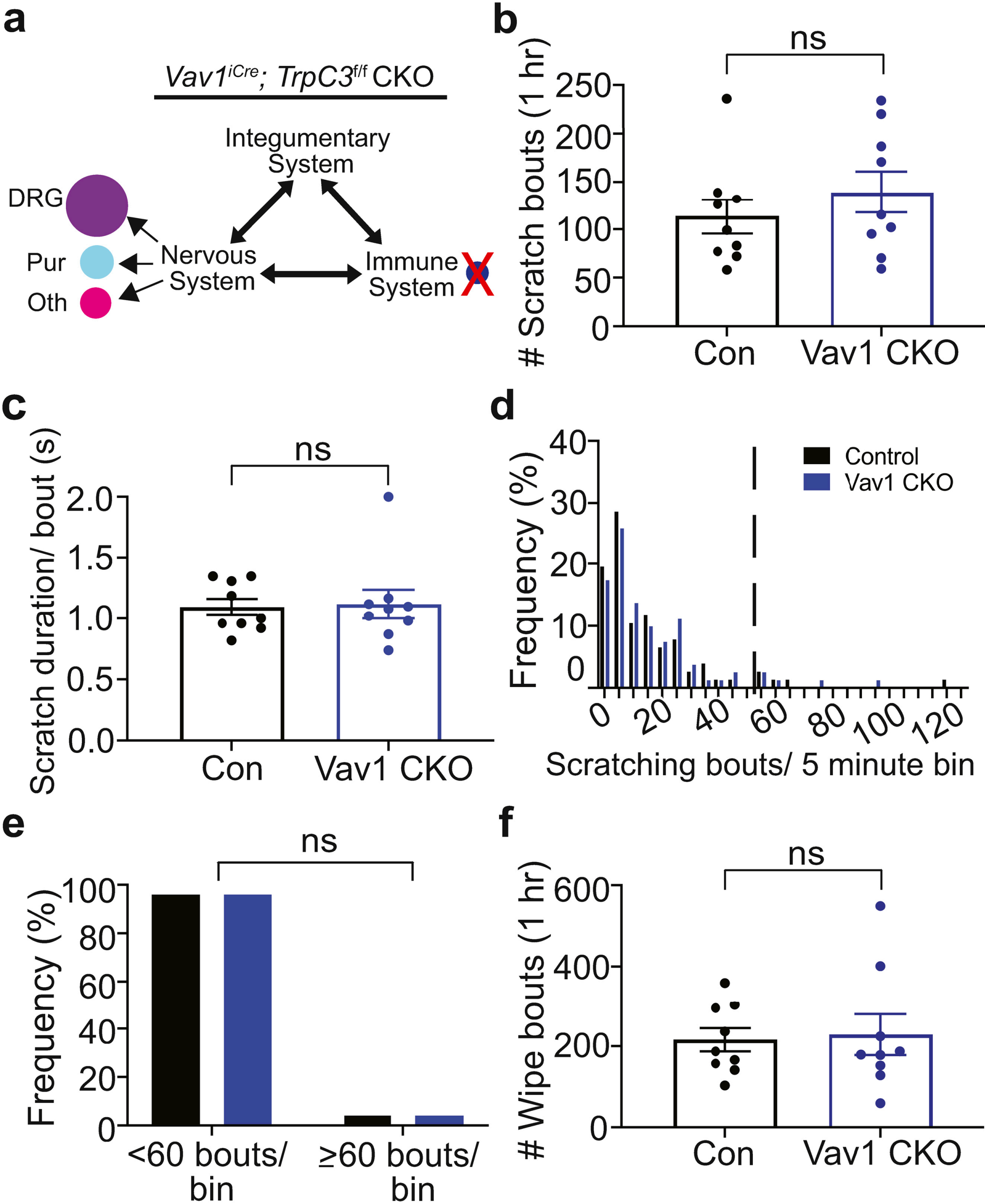
a
Vav1iCre; TrpC3f/f CKO
Integumentary System
DRG
Pur
Oth
Nervous System
Immune System
b
ns
Scratch bouts (1 hr)
250
200
150
100
50
0
Con
Vav1 CKO
c
ns
Scratch duration/ bout (s)
2.0
1.5
1.0
0.5
0.0
Con
Vav1 CKO
d
Frequency (%)
40
30
20
10
0
Control
Vav1 CKO
0
20
40
60
80
100
120
Scratching bouts/ 5 minute bin
e
ns
Frequency (%)
100
80
60
40
20
0
<60 bouts/ bin
≥60 bouts/ bin
f
ns
Wipe bouts (1 hr)
600
400
200
0
Con
Vav1 CKO

a

Mrgd$^{EGFP(+/-)}$

TrpC3 null; *Mrgd*$^{EGFP(+/-)}$

Cervical DRG

IB4/ GFP

CGRP/ GFP

Cerv. Spinal Cord

IB4/ GFP

Treated Skin

CGRP/ GFP

E

D

S

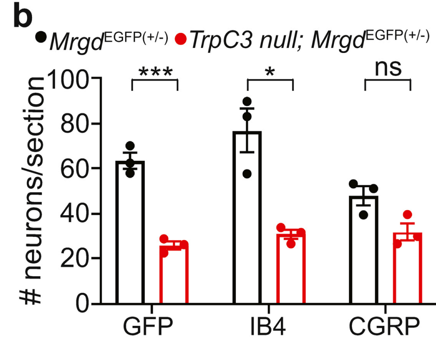

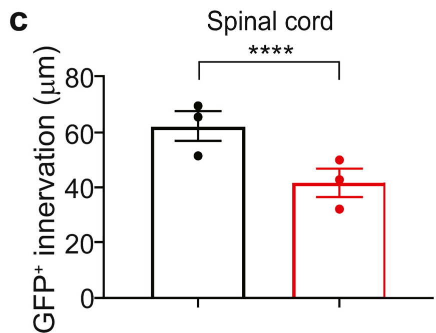

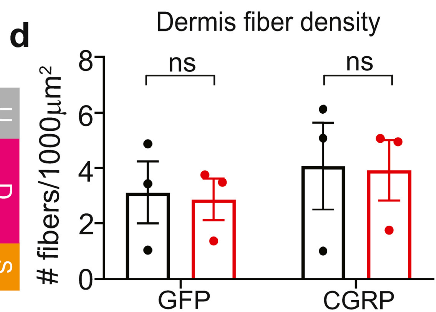

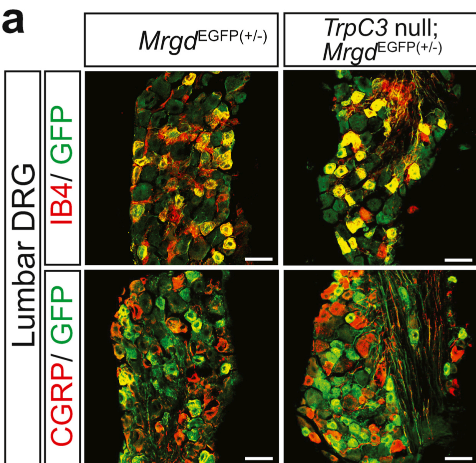
a
Mrgd EGFP(+/-)
TrpC3 null; Mrgd EGFP(+/-)
Lumbar DRG
IB4/ GFP
CGRP/ GFP

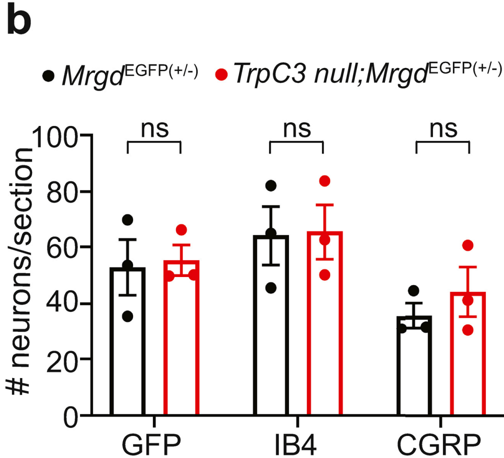
b
Mrgd EGFP(+/-)
TrpC3 null;Mrgd EGFP(+/-)
ns
ns
ns
neurons/section
100
80
60
40
20
0
GFP
IB4
CGRP

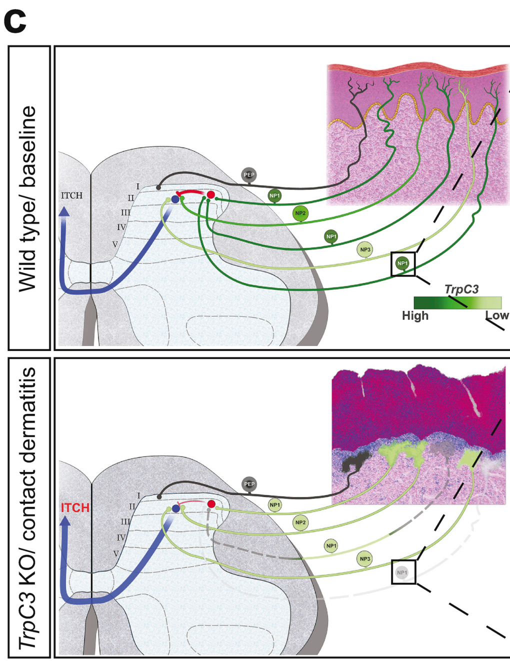
c
Wild type/ baseline
ITCH
I
II
III
IV
V
PEP
NP1
NP2
NP1
NP3
NP1
TrpC3
High
Low
TrpC3 KO/ contact dermatitis
ITCH
PEP
NP1
NP2
NP1
NP3
NP1

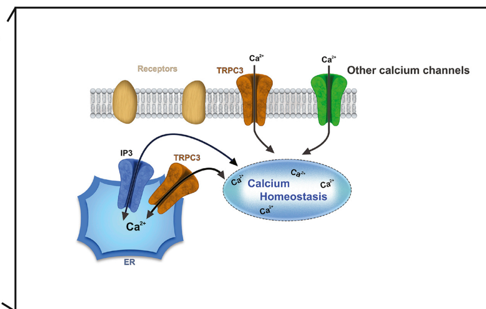
Receptors
TRPC3
Other calcium channels
IP3
TRPC3
Calcium Homeostasis
ER

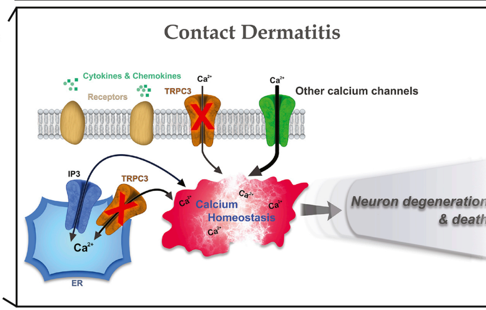
Contact Dermatitis
Cytokines & Chemokines
Receptors
TRPC3
Other calcium channels
IP3
TRPC3
Calcium Homeostasis
Neuron degeneration & death
ER